

Enhancement of the Homogeneity of Micro Slits Prepared by Wire Electrochemical Micromachining

N.S. Qu^{1,2,*}, K. Xu¹, Y.B. Zeng², Qia Yu¹

¹ College of Mechanical and Electrical Engineering, Nanjing University of Aeronautics and Astronautics, Nanjing, China, 210016

² Jiangsu Key Laboratory of Precision and Micro-Manufacturing Technology, Nanjing, China, 210016

Received: 30 July 2013 / *Accepted:* 18 August 2013 / *Published:* 25 September 2013

Wire electrochemical micromachining (WEMM) is promising in the fabrication of metal micro parts or devices because it has many advantages in machining structures with high aspect ratios. The smaller machining gap in WEMM is particularly interesting because higher accuracy can be obtained. However, with such a narrow machining gap, removing electrolysis products and renewing electrolyte become difficult, which would lead to a poor homogeneity of the micro slit. In this paper, the combined method of anode vibration and cathode travelling is used to improve the homogeneity of the micro slits. The influence of the parameters of anode vibration and cathode travelling on the side gap and the homogeneity of micro slits is experimentally investigated. A frequency of 100 Hz with an amplitude of 5 μm and a frequency of 2 Hz with an amplitude of 70 μm are optimal for anode vibration and electrode travelling, respectively. Finally, both groups of micro slits and cantilever curved micro beams with good homogeneity are successfully machined under the optimal conditions.

Keywords: Electrochemical micromachining; Wire electrochemical micromachining; Homogeneity of micro slit; Side gap

1. INTRODUCTION

Micro fabrication plays an increasingly important role in modern industries, such as the aerospace, biomedical, automobile, healthcare and consumer electronics industries [1-3]. Because metal micro structures have desirable properties such as good mechanical strength, magnetic properties, high electrical and thermal conductivities, various techniques have been developed to produce metal micro structures using different principles such as micro milling, micro electrical discharge machining, laser micromachining, ion beam machining, and electrochemical micromachining [4-7]. Electrochemical micromachining is receiving considerable attention to produce metal micro structures because it can electrochemically dissolve conductive materials at atomic sizes

regardless of their hardness and toughness, and it can produce smooth and burr-free surface [8]. Metal micro structures on micrometer and nanometer scales have been achieved using electrochemical micromachining [9-13]. Wire electrochemical micromachining (WEMM) adopts micron-scale wire as a tool cathode because it does not wear out the tool. The metal micro parts and devices are prepared by moving the wire electrode along a programmed path in WEMM [5, 14].

According to the theories in ECM, a smaller side gap corresponds to a higher accuracy in WEMM. Thus, a small machining gap is of great interest. Kim et al. achieved the micrometer-scale side gap and fabricated structures in the hundred-micrometer scale using $\text{\O} 10 \mu\text{m}$ metal wire [15]. Wang et al. reported a $6 \mu\text{m}$ side gap with $\text{\O} 2 \mu\text{m}$ metal wire electrode [16]. Zeng et al. prepared a $0.14 \mu\text{m}$ side gap with $\text{\O} 4 \mu\text{m}$ tungsten wire [17].

Because the gap is deep and narrow in WEMM, it is notably difficult to remove the electrolysis products, namely, the hydroxides and the hydrogen gas, and to renew the electrolyte in the gap. This might lead to poor homogeneity of the machined micro slit. In WEMM, the homogeneity of the machined micro slit has decisive influence on the quality of the micro parts. However, according to our knowledge, there are few publications that concern the homogeneity of micro slits obtained by WEMM. This paper focuses on the homogeneity of micro slits in WEMM. The combined method of vibrating anode with low frequency and travelling cathode in the axial direction of the cathode is introduced to improve the homogeneity of micro slits in WEMM, and the effect of the anode vibration and cathode travelling parameters on the side gap and the homogeneity of the micro slit is experimentally investigated. The optimal parameters are experimentally acquired, and both group of micro slits and cantilever curved micro beams are successfully machined.

2. EXPERIMENTAL

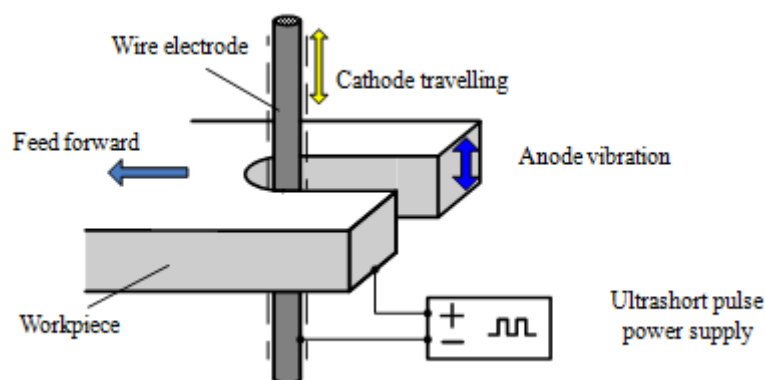


Figure 1. Schematic diagram of WEMM in this experiment

Figure 1 shows the principle of WEMM. An ultrashort-pulse power supply is applied between the electrodes in an electrolyte cell, and the wire electrode (cathode) moves towards the workpiece (anode). In this study, the combined method of anode vibration and cathode travelling during the processing is used, as shown in Figure 1. The anode vibration decreases the accumulation of insoluble

electrolysis products near the workpiece. The cathode travelling drives the electrolyte flow in the machining area, which helps the renewing of the electrolytes and the removal of the electrolysis products, such as bubbles and insoluble electrolysis products. Figure 2 shows the experimental setup, which consists of a servo-control feed unit, a power supply, electrodes, an electrolyte cell and a PZT (piezoelectric ceramics) unit. A wire electrode is attached to a three-axis stage with a 0.1 μm resolution, which can achieve the feed movement and the wire electrode travelling in the machining process. An ultrashort-voltage-pulse power supply is used to produce durations of a few tens of nanoseconds, and the current waveforms are monitored using an oscillograph. The electrolyte cell, which is connected to the workpiece by a fixture, is positioned on a vibration table driven by PZT. When the PZT is charged by the pulses that are produced by the PZT controller, the vibration of the workpiece occurs with a low frequency.

Tungsten wire with 4 μm diameter (Goodfellow, Corp.) is adopted as a tool electrode. The tungsten wire is insulated with silastic except the machining area. A cobalt-base alloy with a thinness of 80 μm is adopted as the workpiece. Diluted hydrochloric acid with a concentration of 0.05 M is preferred as the electrolyte because the acid electrolyte usually produces much less insoluble electrolysis products than common salt electrolytes, which is important when the side gap is so tiny. In all of the experiments and featured fabrication, the wire electrode feedrate is set at 0.2 $\mu\text{m s}^{-1}$.

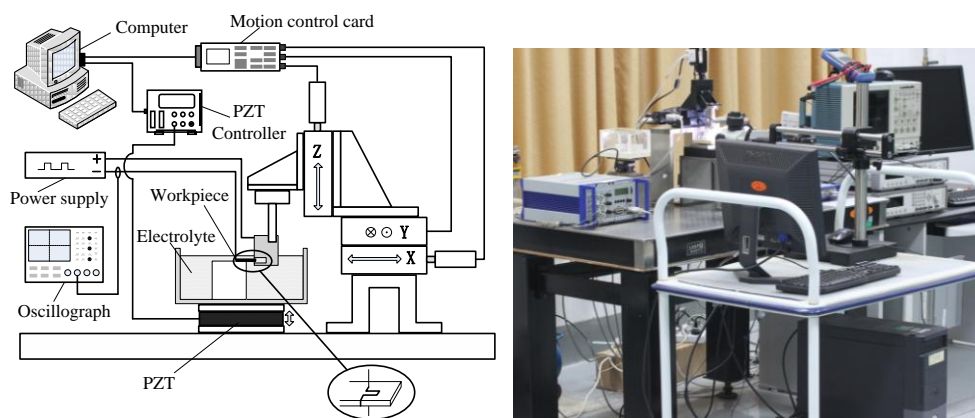


Figure 2. Experimental setup

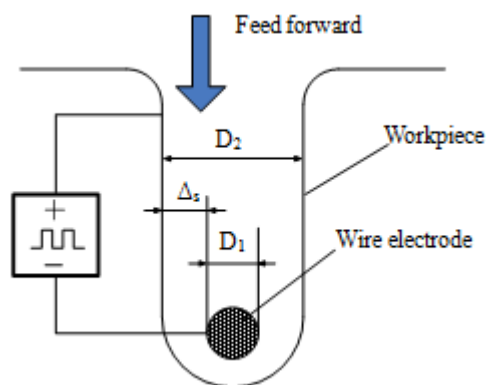


Figure 3. Side gap in WEMM

Figure 3 illustrates the machining gap in WEMM. The side gap Δ_s is defined by

$$\Delta_s = \frac{D_2 - D_1}{2} \quad (1)$$

where D_1 is the diameter of the wire electrode, and D_2 is the width of the machined micro slit.

The width of the slits was measured using a digital microscope (DVM5000, Lecia, Germany). Ten measurements were taken for each sample, and an average slit width value was calculated. A scanning electron microscope (S-3400N, Hitachi, Japan) was used to observe the machined micro slit.

3. RESULTS AND DISCUSSION

3.1 Determination of the anode vibration parameters

Figure 4 shows the influence of the anode vibration frequency on the side gap, which was obtained at an anode vibration amplitude of 5 μm , a cathode travelling frequency of 2 Hz, a cathode travelling amplitude of 70 μm , a pulse period of 6 μs , a voltage of 6 V, and a pulse duration of 30 ns. Figure 4(a) indicates that the average side gap decreases gradually with the anode vibration frequency when the frequency ranges from 20 to 60 Hz; then, the side gap reversely reduces with a further increase in anode vibration frequency from 60 to 180 Hz. The minimum side gap of 0.60 μm is observed at the anode vibration frequency of 60 Hz. Note that the deviation range of the side gap also varies with a rise in the anode vibration frequency. In the present experiments, the maximum deviation range of 1 μm is observed at the anode vibration frequency of 60 Hz, and the minimum deviation range of 0.21 μm is observed at the anode vibration frequency of 100 Hz. Although the average side gap is only 0.60 μm , the maximum side gap is 1.25 μm at the anode vibration frequency of 60 Hz. However, the maximum side gap is only 0.78 μm although the average side gap is 0.65 μm at the anode vibration frequency of 100 Hz.

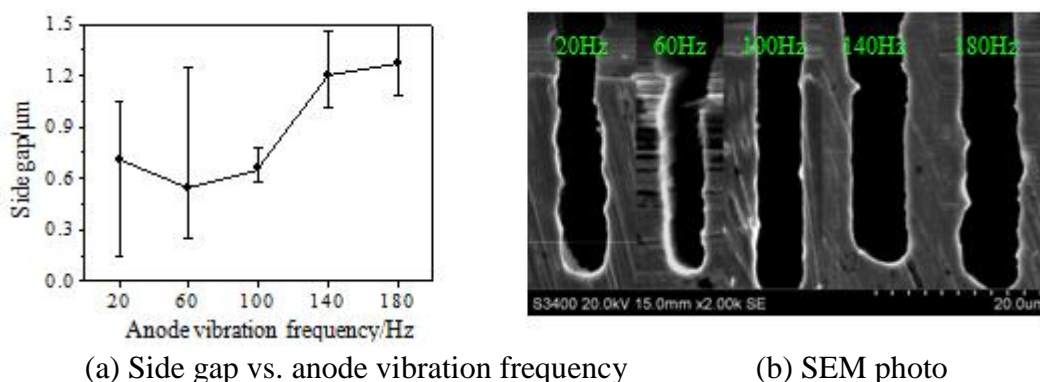


Figure 4. Effect of the anode vibration frequency on the side gap (anode vibration amplitude: 5 μm , cathode travelling frequency: 2 Hz, cathode travelling amplitude: 70 μm)

Therefore, a frequency of 100 Hz is optimal for anode vibration. As shown in Figure 4(b), the micro slit that was prepared with an anode vibration frequency of 100 Hz has the best homogeneity

among the five micro slits. Bhattacharyya et al. also reported that low-frequency vibration significantly increases accuracy during micro-machining operation of copper test pieces and high-frequency vibration has no significant effect on accuracy[18].

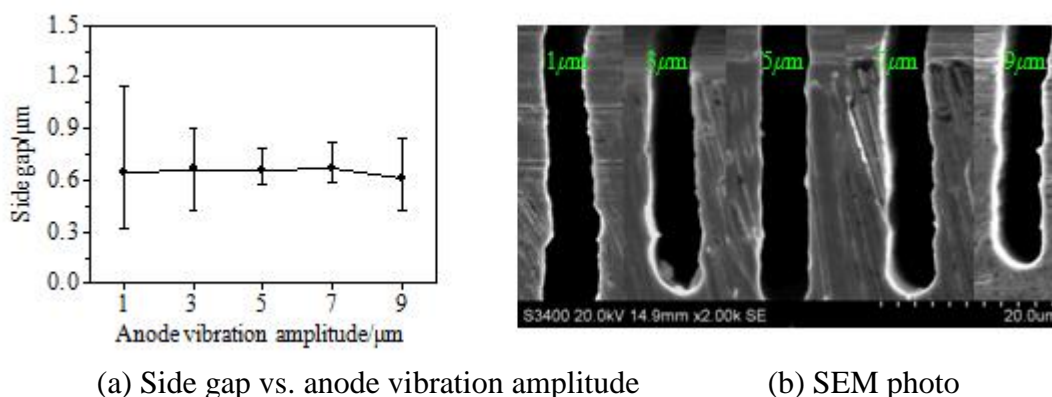


Figure 5. Effect of the anode vibration amplitude on the side gap (anode vibration frequency: 100 Hz, cathode travelling frequency: 2 Hz, cathode travelling amplitude: 70 μm)

The influence of the anode vibration amplitude on the side gap is illustrated in Figure 5 for the micro slits that were obtained at an anode vibration frequency of 100 Hz, a cathode travelling frequency of 2 Hz, a cathode travelling amplitude of 70 μm , a pulse period of 6 μs , a voltage of 6 V, and a pulse duration of 30 ns. Figure 5(a) denotes that the anode vibration amplitude has little effect on the side gap. However, the anode vibration amplitude has significant effect on the deviation range of micro slits. The micro slit that was prepared with anode vibration amplitude of 5 μm has the best homogeneity among the five micro slits, as shown in Figure 5(b). Therefore, the anode vibration amplitude of 5 μm is optimal for anode vibration. In fact, there is no report related to the effect of anode vibration amplitude on side gap in previous reports, and this paper first demonstrates the effect of anode vibration amplitude on side gap.

3.2 Determination of the cathode travelling parameters

The effect of the cathode travelling parameters on the side gap is also investigated. Figure 6 shows the influence of the cathode travelling amplitude on the side gap that was obtained at an anode vibration amplitude of 5 μm , an anode vibration frequency of 100 Hz, a cathode travelling frequency of 2 Hz, a pulse period of 6 μs , a voltage of 6 V, and a pulse duration of 30 ns. Figure 6(a) indicates that the average side gap increases gradually with the cathode travelling amplitude, which ranges from 10 to 100 μm . The deviation range of the side gap also varies with a rise in the cathode travelling amplitude. The deviation range for the cathode travelling amplitudes of 10 and 40 μm is bigger than that for the cathode travelling amplitudes of 70 and 100 μm , and the deviation range for the cathode travelling amplitudes of 70 and 100 μm is almost identical. Figure 6(b) shows that the micro slit that

was prepared with the cathode travelling amplitude of 70 μm has the best homogeneity among these micro slits.

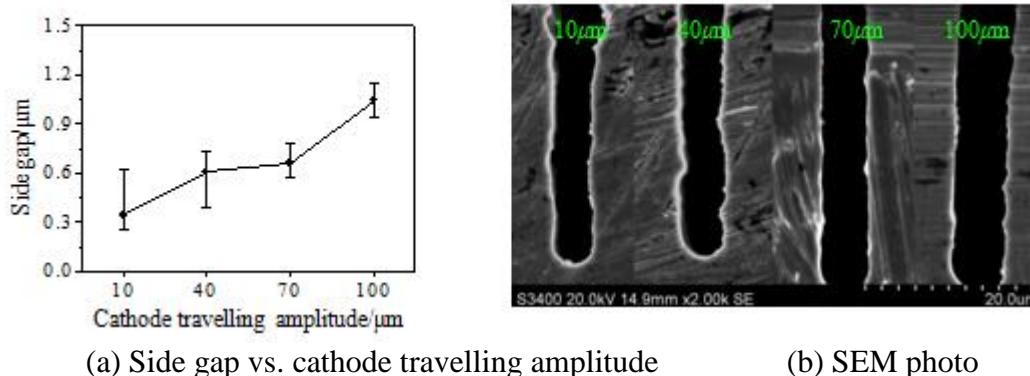


Figure 6. Effect of the cathode travelling amplitude on the according side gap (cathode travelling frequency: 2 Hz, anode vibration frequency: 100 Hz, anode vibration amplitude: 5 μm)

The influence of the cathode travelling frequency on the side gap is illustrated in Figure 7 for the micro slits that were obtained at an anode vibration amplitude of 5 μm , an anode vibration frequency of 100 Hz, a cathode travelling amplitude of 70 μm , a pulse period of 6 μs , a voltage of 6 V, and a pulse duration of 30 ns. Figure 7(a) indicates that the average side gap increases gradually with the cathode travelling frequency, which ranges from 1 to 2 Hz; then, the side gap slightly changes with a further increase in cathode travelling frequency from 2 to 5 Hz. The minimum deviation range of the side gap occurs at the cathode travelling frequency of 2 Hz. The micro slit that was prepared at the cathode travelling frequency of 2 Hz has the best homogeneity among the five micro slits, as shown in Figure 7(b). Therefore, a frequency of 2 Hz and an amplitude of 70 μm are optimal for cathode travelling.

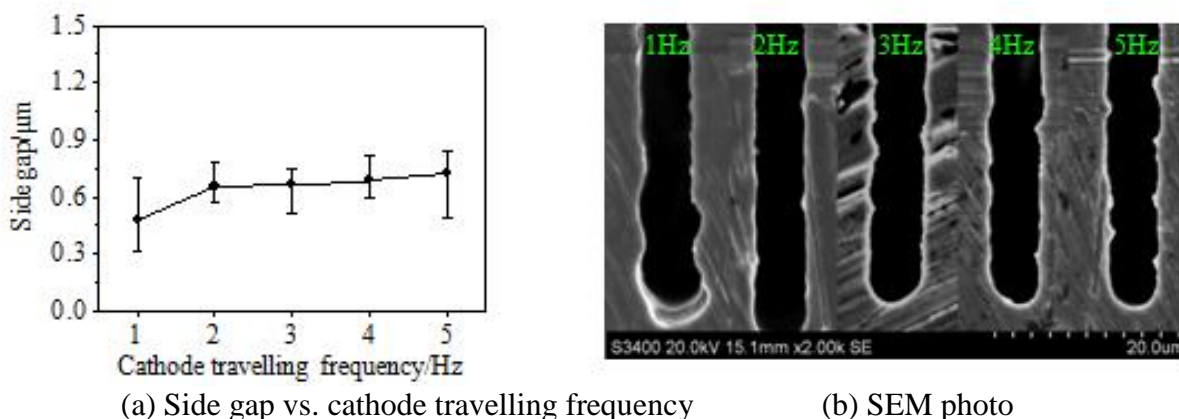


Figure 7. Side gap according to the cathode travelling frequency (cathode travelling amplitude: 70 μm , anode vibration frequency: 100 Hz, anode vibration amplitude: 5 μm)

3.3 Determination of the applied voltage

Figure 8 shows the effect of the applied voltage on the side gap that was obtained at an anode vibration amplitude of 5 μm , an anode vibration frequency of 100 Hz, a cathode travelling amplitude of 70 μm , a cathode travelling frequency of 2 Hz, a pulse period of 6 μs , and a pulse duration of 30 ns. Figure 8(a) indicates that the average side gap increases as the applied voltage increases. A large voltage leads to a high current density, which induces a high material-removing rate; then, a wide side gap is obtained. However, the deviation range of the side gap varies with an increase in the applied voltage. The minimum deviation range of the side gap occurs at an applied voltage of 5.8 V. As shown in Figure 8(b), the micro slit that was machined at the applied voltage of 5.8 V shows the best homogeneity. Kim et al. also indicated that the applied voltage of 6 V is helpful to acquire small side gap [14].

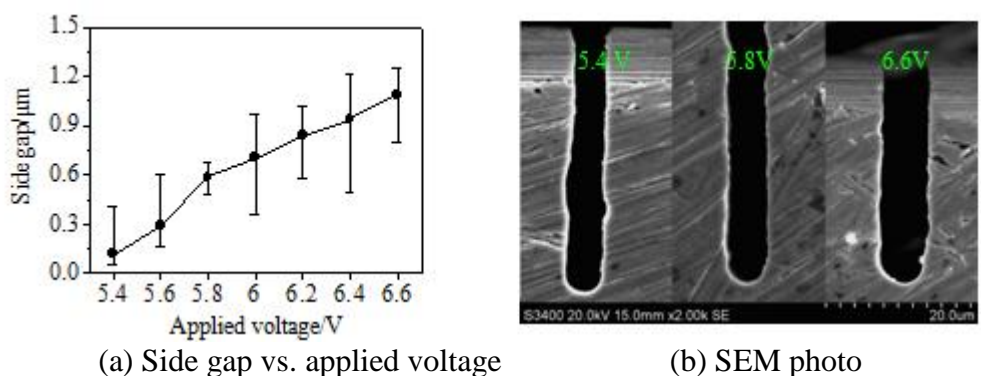


Figure 8. Effect of the applied voltage on the side gap (pulse period: 6 μs , pulse duration: 30 ns)

3.4 Determination of the pulse duration

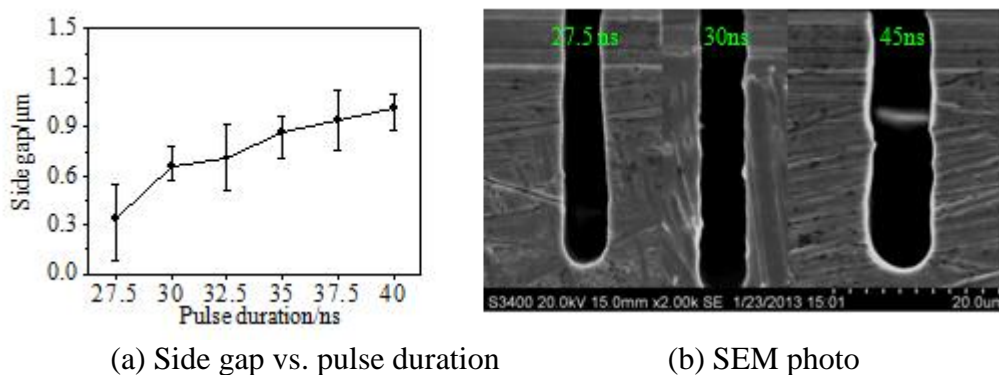


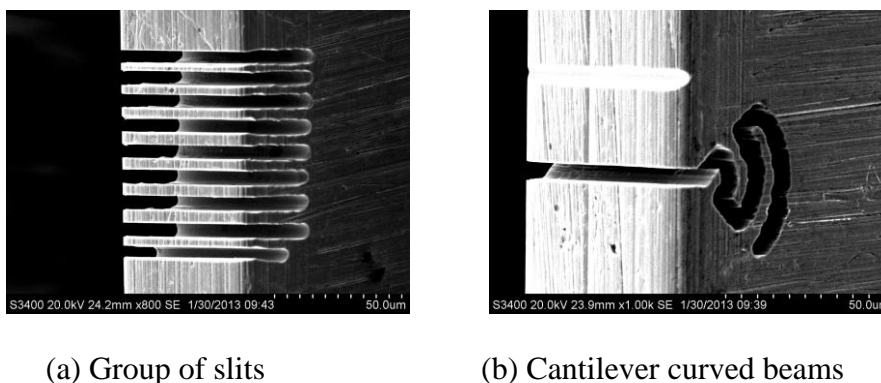
Figure 9. Effect of the pulse duration on the side gap (pulse period: 6 μs , voltage: 6 V)

Figure 9 demonstrates the effect of the pulse duration on the side gap at an anode vibration amplitude of 5 μm , an anode vibration frequency of 100 Hz, a cathode travelling amplitude of 70 μm , a cathode travelling frequency of 2 Hz, a voltage of 6 V, and a pulse period of 6 μs . It is noted that the average side gap increases with a rise in the pulse duration. When the pulse duration is longer than 40

ns, the side gap is larger than 1 μm . This result is attributed to the increase in the actual machining time. Therefore, the pulse duration of 30 ns is optimal for WEMM with a sub-micrometer scale side gap. This result is not agreed with the report by Kim et al. [14]. This could attribute to enhancement of renewing the electrolyte in the present study.

3.5 Fabrication of micro structures

Various features are fabricated using the optimal machining parameters that are determined in the basic experiments. Figure 10(a) shows a group of slits and a group of beams, and Figure 10(b) shows the cantilever curved beams that were machined with side gaps in the sub-micrometer scale. The width of each beam and the slit beams in Figure 10 is approximately 5 μm . The aspect ratio is approximately 15.



(a) Group of slits

(b) Cantilever curved beams

Figure 10. Microstructures that were fabricated on cobalt-base alloys with 5 μm , 100 Hz anode vibration and 70 μm , 2 Hz cathode travelling. (Applied voltage: 5.8 V, pulse duration: 30 ns, pulse period: 6 μs).

4. CONCLUSIONS

In this paper, the influence of the anode vibration and cathode travelling parameters on the side gap and the homogeneity of micro slits is investigated in WEMM. The frequency of 100 Hz with an amplitude of 5 μm and the frequency of 2 Hz with an amplitude of 70 μm are optimal for anode vibration and electrode travelling, respectively. The experiments also show that the applied voltage and the pulse duration significantly influence the side gap width in WEMM. A low applied voltage and a short pulse duration might lead to a narrow side gap. Finally, micro features with good shape are machined using the optimal machining parameters.

ACKNOWLEDGMENTS

This work was financially supported by the National Natural Science Foundation of China (91023018).

References

1. K. P. Rajurkar, G. Levy, A. Malshe, M. M. Sundaram, J. A. McGeough, X. Hu, R. Resnick and A. DeSilva, *Cirp. Ann.-Manuf. Techn.* 55 (2) (2006) 643.
2. E. J. W. Berenschot, H. V. Jansen and N. R. Tas, *J. Micromech. Microeng.* 23 (5) (2013) 055024.
3. D. G. Courtney, H. Q. Li and P. C. Lozano, *J. Microelectromech. S.* 22 (2) (2013) 471.
4. J. Kozak, K. R. Rajurkar, and Y. Makkar, *J. Mater. Process. Techn.* 149 (2004) 426.
5. D. Zhu D, K. Wang and N. S. Qu, *Cirp. Ann.-Manuf. Techn.* 56 (1) (2007) 241.
6. P. Rodriguez and J. E. Labarga, *J. Mater. Process. Techn.* 213 (2) (2013) 261.
7. M. D. Nguyen, M. Rahman and Y.S. Wong, *Appl. Surf. Sci.* 69 (2013) 48
8. B. H. Kim, C.W. Na, Y. S. Lee, D. K. Choi and C. N. Chu, *Cirp. Ann.-Manuf. Techn.* 54 (1) (2005) 191
9. R. Schuster, V. Kirchner, P. Allongue and G. Ertl, *Sci.* 289 (5476) (2000) 98.
10. R. Schuster, *ChemPhysChem.* 8 (2007) 34.
11. E. L. Hotoiu, S. Van Damme, C. Albu, D. Deconinck, A. Demeter and J. Deconinck, *Electrochim. Acta.* 93 (2013) 8
12. P. Raffelstetter and B. Molloy, *Electrochim. Acta.* 55 (6) (2010) 2149
13. O. Zinger, P. F. Chauvy and D. Landolt, *J. Electrochem. Soc.* 150 (11) (2003) B495
14. H. S. Shin, B. H. Kim and C. N. Chu, *J. Micromech. Microeng.* 18 (7) (2008) 1
15. B. J. Park, B. H. Kim and C. N. Chu, *Cirp. Ann.-Manuf. Techn.* 55 (1) (2006) 197
16. S. H. Wang, D. Zhu, Y. B. Zeng and Y. Liu, *Int. J. Adv. Manuf. Technol.* 53 (2011) 535
17. Y. B. Zeng, Y. Liu, S. H. Wang and D. Zhu, *Cirp. Ann.-Manuf. Techn.* 61 (1) (2012) 19
18. B. Bhattacharyya, M. Malapati, J. Munda and A. Sarkar, *Int. J. Mach. Tool. Manu.* 47 (2007) 335–342